Available online at www.sciencedirect.com

ScienceDirect

IFAC PapersOnline CONFERENCE PAPER ARCHIVE

IFAC PapersOnLine 53-2 (2020) 16269–16274

Rayleigh Damping Modelling for Tumor Detection using Digital Image Elasto Tomography (DIET)

Jessica. L Fitzjohn * **Cong Zhou** * **J. Geoffrey Chase** *
Zane Ormsby ** **Marcus Haggers** **

* *Department of Mechanical Engineering, Centre for Bio-engineering, University of Canterbury, Christchurch, New Zealand (e-mail: jessica.fitzjohn@pg.canterbury.ac.nz, cong.zhou@canterbury.ac.nz, geoff.chase@canterbury.ac.nz)*
** *Tiro Medical, Christchurch, New Zealand (e-mail: zane.ormsby@tiromedical.com, marcus.haggers@tiromedical.com)*

Abstract: This study develops a model based on Rayleigh Damping (RD) with potential use in breast cancer diagnostics. Displacement data of over 14,000 reference points on the breast surface from 14 breasts was captured using the Digital Image Elasto Tomography (DIET) system. The reference points were split into four segments and an ellipse fit utilized to calculate the work done and consequent viscous damping constant for each reference point. Fitting a model based on RD to median filtered data gave consistent results for one model coefficient across all breasts. The other coefficient was seen to have diagnostic potential when the model was fit to unfiltered data, and is the focus of this paper. The coefficient value was compared between breast segments adjacent to and containing the tumor (locations given from X-ray mammography) to those opposite the tumor. A total of 11 out of 14 breasts had a higher coefficient found in the tumor segment and all breasts had a higher coefficient in at least one adjacent segment. This method showed potential for breast specific diagnosis and tumor localisation using the DIET system.

Keywords: Tumor detection, Breast cancer, Viscous damping, Digital Imaging, DIET

1. INTRODUCTION

Breast cancer is the leading cause of cancer deaths in women worldwide (van den Ende et al., 2017; Lotz et al., 2011). Annual diagnosis is estimated at over 1 million women with approximately 400,000 mortalities (Coughlin and Ekwueme, 2009). Early detection of breast cancer greatly increases 5-year survival rates to over 95% due to increased treatment options (Heywang-Kbrunner et al., 2011). This demonstrates the need for affordable breast cancer screening programs worldwide.

X-ray mammography is currently widely used for breast cancer screening. This technique is controversial due to painful breast compression and harmful radiation exposure (van den Ende et al., 2017). It thus results in poor compliance and a limited age bracket for screening. The success of mammography is also dependent on the experience of the radiologist, and a small variation (5-10%) in radio density between healthy and cancerous tissue leads to false positives and over diagnosis (Elmore et al., 2002). Mammography screening is also high cost and is of limited availability in developing countries.

Digital Image Elasto Tomography (DIET) (Peters et al., 2004, 2008, 2005) is a low cost alternative breast cancer screening approach, which uses the significant contrast in elastic properties (400-1000%) of healthy and cancerous tissue (Abbas et al., 2007). The DIET system consists of an actuator, which induces a steady state sinusoidal vibration in the breast at a range of input frequencies. Surrounding cameras capture images of the breast surface motion which are then analysed using surface volume and optical flow techniques. This approach results in displacement data for approximately 14,000 reference points on the breast surface. Analysis of this data has yielded reasonable diagnostic success including Zhou et als study on hysteresis loop analysis (HLA) (Zhou et al., 2018). However, this method was tested using silicone phantoms with homogeneous properties and was not validated using clinical data with higher complexity.

This paper develops a computationally simple method of assessing viscous damping properties in breast tissue with diagnostic potential. It fits a model based on the Rayleigh damping model to equivalent viscous damping coefficients analysed for numerous reference points segmented on the breast surface. Assessment of one of the model coefficients shows its ability to distinguish between breast segments containing a tumor and those in an opposite segment. This result shows the potential of the method to provide not only a diagnostic but also tumor localisation. The method was tested with real data from 13 different subjects (a total of 14 breasts with a tumor) involved in a clinical trial with Canterbury Breast Care.

10.1016/j.ifacol.2020.12.626

2. METHOD

2.1 Clinical Data

13 women diagnosed with breast cancer via mammography at Canterbury Breast Care (Christchurch, NZ) were recruited to undergo testing with a prototype DIET system, as part of an ongoing larger clinical trial. Ethics approval for the experimental tests, data collection, and analysis of this data was granted by the NZ National Health and Disability Ethics Committee, South Island Regional Committee.

12 women had cancer in one breast and one women had cancer in both breasts, with a total of 14 breasts used for this first analysis. Tumor sizes ranged from 7 to 48mm and displacement data was available for a range of testing frequencies between 20 and 100Hz. Table 1 shows the size and tumor location for each patient.

Table 1. Tumor size and locations for patients

Subject	Tumor Diameter (mm)	Location
P1	12	Left 6 o'clock
P2	8	Left 9 o'clock
P3	18	Left 10 o'clock
P4	15	Left 2.30 o'clock
P5	14	Right 10 o'clock
P6	14	Left 12.30 o'clock
P7	48	Left 3-5 o'clock
P8	7	Left 9-12 o'clock
P9	7.5	Right 10 o'clock
P10	10	Left 11 o'clock
P11	37	Right 10.30 o'clock
P12	14	Left 11 o'clock
P13.1	11	Left 2 o'clock
P13.2	12	Right 10 o'clock

2.2 Viscous Damping in Breast Tissue

The displacement data for approximately 14,000 reference points on the breast surface was provided by Tiro Medical (Christchurch, New Zealand) and split radially into four columns. The breasts were segmented to ensure the known tumor location, found via x-ray mammography, was contained in the centre of one segment, resulting in a tumor segment, two adjacent segments and one opposite ("healthy") segment. The segmentation method is shown in Fig. 1.

Each reference point on the breast surface was modelled as a viscous damper with a viscous damping constant calculated using Equation (1).

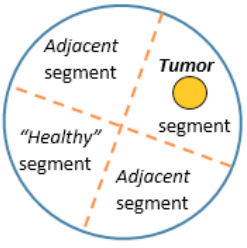

Fig. 1. Schematic of breast segmentation method showing tumor location

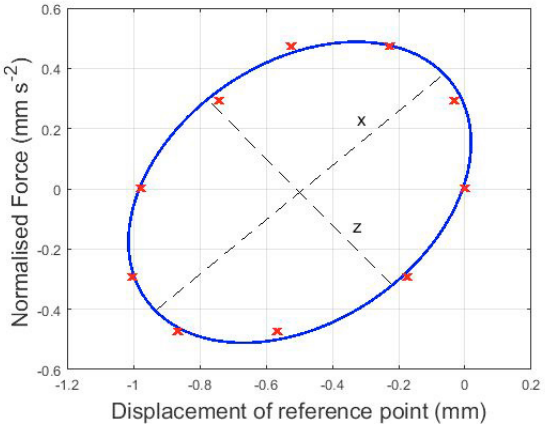

Fig. 2. Ellipse fit for a single reference point with major and minor axes shown

$$C_{eq} = \frac{W_d}{\pi \omega X^2}. \tag{1}$$

Where ω is the input frequency and X is the response amplitude found from fitting a sine wave to the displacement-time data. W_d is the work done, which was calculated using the area of an ellipse fitted to the force-displacement plot for each reference point (see Fig. 2). The force, F, is the sinusoidal input force normalised by mass in Equation (2) and Equation (3) shows the ellipse area calculation for work done using the major and minor ellipse axes, 'x' and 'z'.

$$F = 0.5sin(\omega t) = 0.5sin(2\pi f t) \tag{2}$$

$$W_d = \pi x z \tag{3}$$

The damping constant was calculated for each reference point and plotted against the major axis of the ellipse for each separate segment.

2.3 Damping Model based off Rayleigh Damping

Rayleigh damping (RD) is often used to model structural damping in seismic analysis of buildings (Petrov et al., 2015). It is proportional to a linear combination of mass and stiffness and results in different damping ratios for different response frequencies, according to:

$$\zeta = \frac{1}{2}(\frac{\mu}{\omega} + \lambda\omega) \tag{4}$$

Where μ and λ are mass and stiffness proportional constants respectively. A diagram of the nature of the RD curve is shown in Fig. 3 showing the mass and stiffness contributions to the curve shape.

Observations of the equivalent viscous damping constants in each segment plotted against the major axis of the force-displacement ellipse closely resembled that of a RD curve across all subjects. This outcome illustrated the potential to infer breast tissue properties and viscous behaviour by implementing a model similar to RD. The damping model used to describe the trend of data points in each breast is defined:

$$C_{eq} = \frac{a}{x} + bx \tag{5}$$

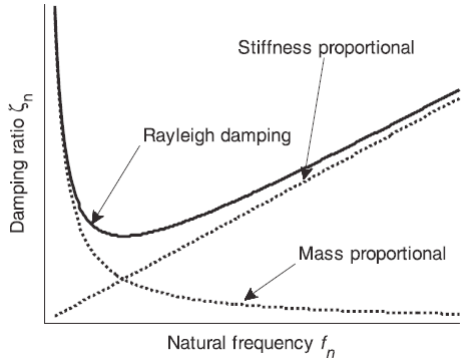

Fig. 3. Rayleigh damping curve showing mass and stiffness contributions

where a and b are breast and frequency specific coefficients and x is the length of the major axis of the force-displacement ellipse. This model can be used to determine consistent properties of breast tissue and has the potential to provide a computationally simple diagnostic technique.

2.4 'B' coefficient Analysis

The 'a' coefficient of the damping model is comparable to the mass proportional constant in RD. Assessment of the 'a' coefficients showed very high consistency across all breasts, which gives potential to infer general properties of breast tissue. The 'b' coefficient is related to stiffness, which is expected to vary with the presence of a tumor due to the significant contrast in elastic properties between healthy and cancerous tissue. Therefore, there is potential for this model term to have diagnostic capabilities.

Prior to analysis, large outliers were excluded by limiting x to between 0 and 0.1 and excluding overdamped points with equivalent viscous damping $\zeta > 1$. A median filter with window size of 5 was applied to the data before fitting the damping model to find the 'a' coefficients describing the 'back bone' of the curve. It should be noted, applying the damping model to the median filtered data is unlikely to yield any diagnostic results, as the observed effect of tumors tend to lie in points not displaying the common trend.

Thus, to analyse diagnostic capabilities of this model, the effect of outliers on the 'b' coefficient was assessed using unfiltered data, and restricting the 'a' term to within $a \pm 0.0001$ of the median filtered 'a' value. It was hypothesised the 'b' coefficients in cancerous segments would be higher due to more outliers with higher damping, showing their higher local stiffness.

To test this theory, the 'b' coefficient found in the *"healthy"* segment opposite the tumor was compared to that of the cancerous and adjacent segments. Thus, this first analysis assessment is breast specific, removing the impact of variances amongst breasts in the subjects. Breast specific methods are preferable to those which compare two breasts from the same subject. Breast comparison methods could lead to false negatives when patients have a tumor in each breast, as is the case with one of the patients in this proof of concept study.

3. RESULTS

Figs. 4 and 5 show a comparison of 'b' coefficients between the four segments in the cancerous breasts of different subjects at available frequencies. The dotted line was used to assess whether the 'b' coefficients in segments containing the known tumor location and adjacent to it are larger than those in the segment furthest from the tumor. Zero values sometimes occurred when subjects were missing data for some input frequencies, arising due to issues in optical flow and image reconstruction. Fig. 6 shows the results for all subjects in Figs. 4 and 5 averaged across frequency.

4. DISCUSSION

Of the 14 cancerous breasts analysed in Fig. 4 and 5, 10 were found to have the majority of 'b' coefficients in the cancerous and adjacent segments higher than those in the "healthy" segment. Subjects P1, P3, P5, and P7 presented with 'b' coefficients consistently above the line; subject P4, was considered average with an equal amount of points above and below the threshold line and three were considered poor: P6, P10 and P13.1.

Of the three considered poor all had comparatively small tumors with diameters 14, 10 and 11mm for P6, P10 and P13.1, respectively. A smaller tumor would be expected to have less of an effect on surrounding tissue properties and perhaps not present as well in this type of method. Subjects P4 and P13.1 were also missing some analysis frequencies, which could effect the results.

Fig. 6 showing all subjects' results averaged in frequency shows most subjects had higher 'b' values associated with the tumor segment than the "healthy" segment. For those subjects that did not, all had at least one *adjacent* segment with a higher b coefficient. First, this result shows surrounding tissue is affected by the presence of a tumor. Second, it should be noted tumor localisation using mammography can be difficult and error prone and thus given tumor locations are estimates. Segments identified as adjacent to the tumor are not unlikely to be the actual tumor location. Hence, their consideration in this analysis.

Fig. 6 also shows a large variation in 'b' values in general across the 14 breasts. This variability demonstrates how diagnosis based on a generalized threshold value is often less robust, due to the large variation in breast size and density, across even small cohorts. Comparing breast properties with other regions in the *same* breast, as with this method, removes this issue. One such issue in mammography is the limited success in detecting tumors in denser breasts. Development of standardised patient specific methods such as these will have significant benefit.

5. CONCLUSION

The results of this proof of concept study show a greater model 'b' coefficient in tumor and adjacent segments than in the healthy segment for the 14 breasts analysed. This therefore has potential to be used as a diagnostic tool for breast cancer diagnosis. Further validation of the success of this method would include identification of tumor locations in a randomized cohort.

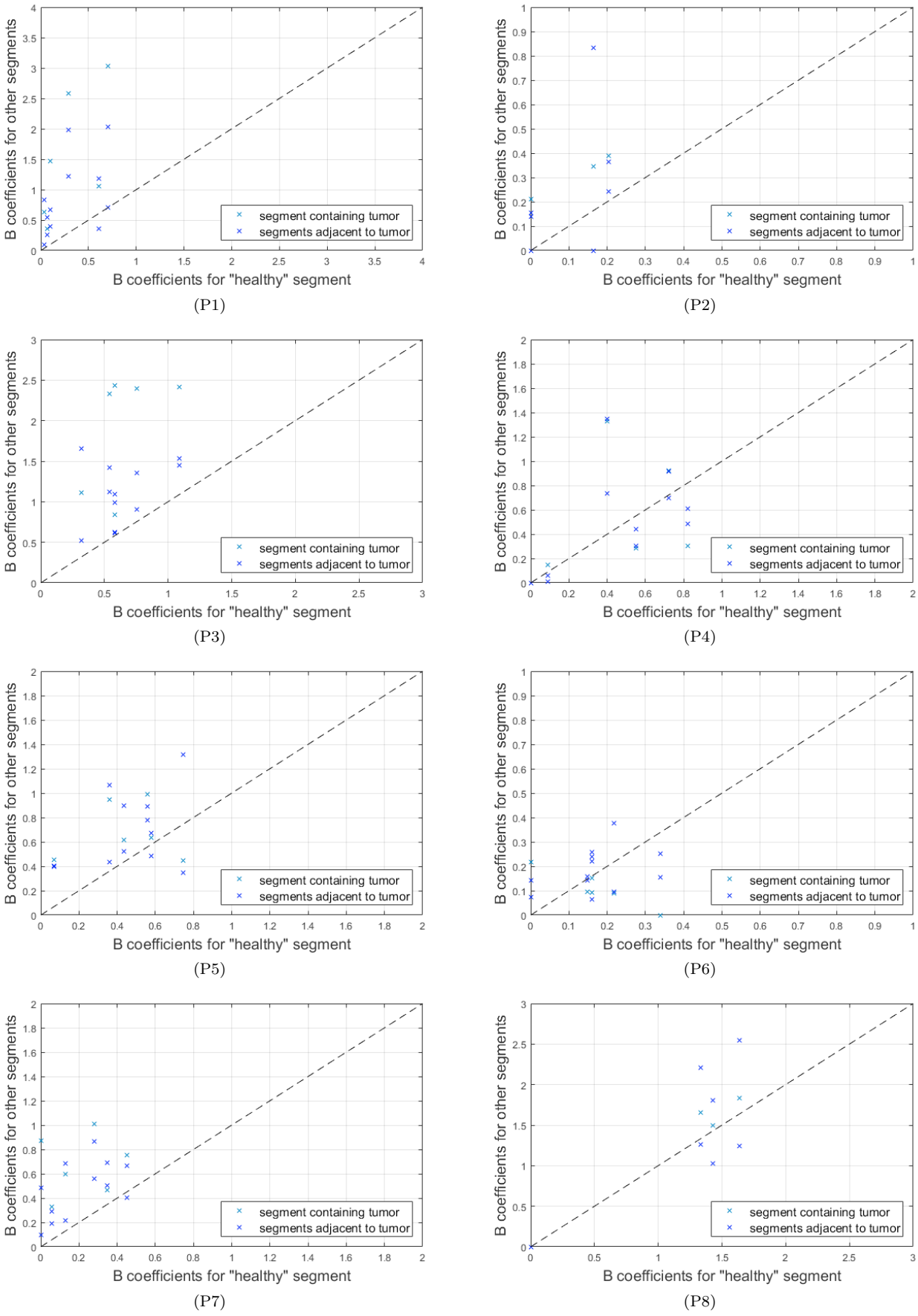

Fig. 4. Comparison of B coefficients in "healthy" and tumor segments for Patients 1-8

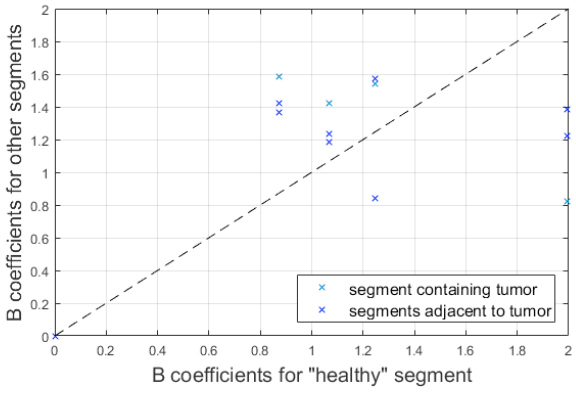

(P9)

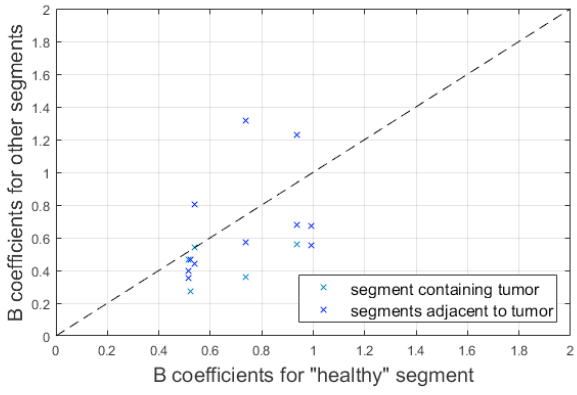

(P10)

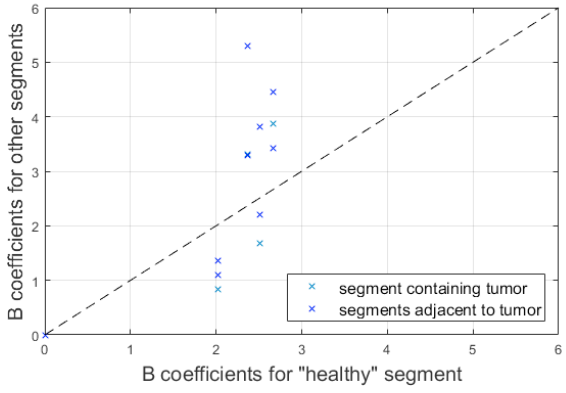

(P11)

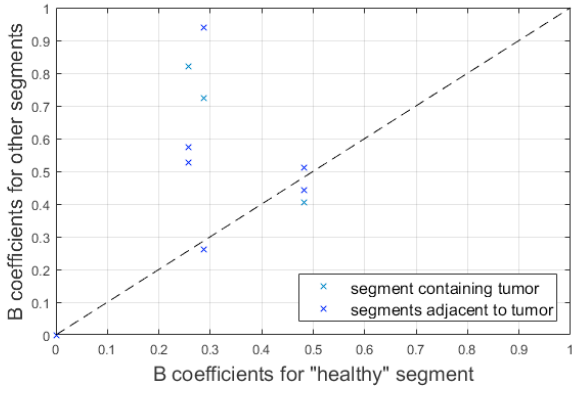

(P12)

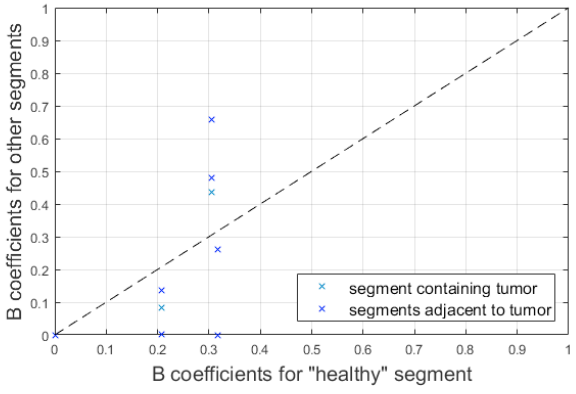

(P13.1)

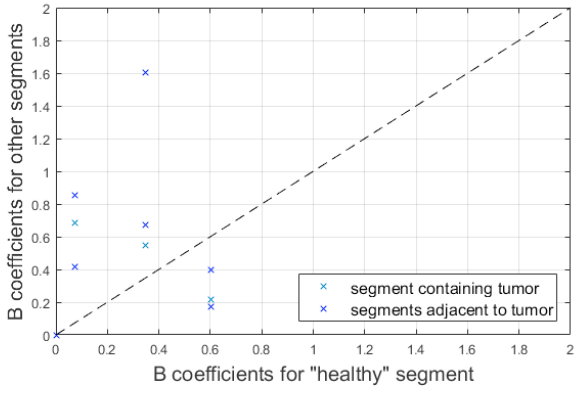

(P13.2)

Fig. 5. Comparison of B coefficients in "healthy" and tumor segments for Patients 9-14

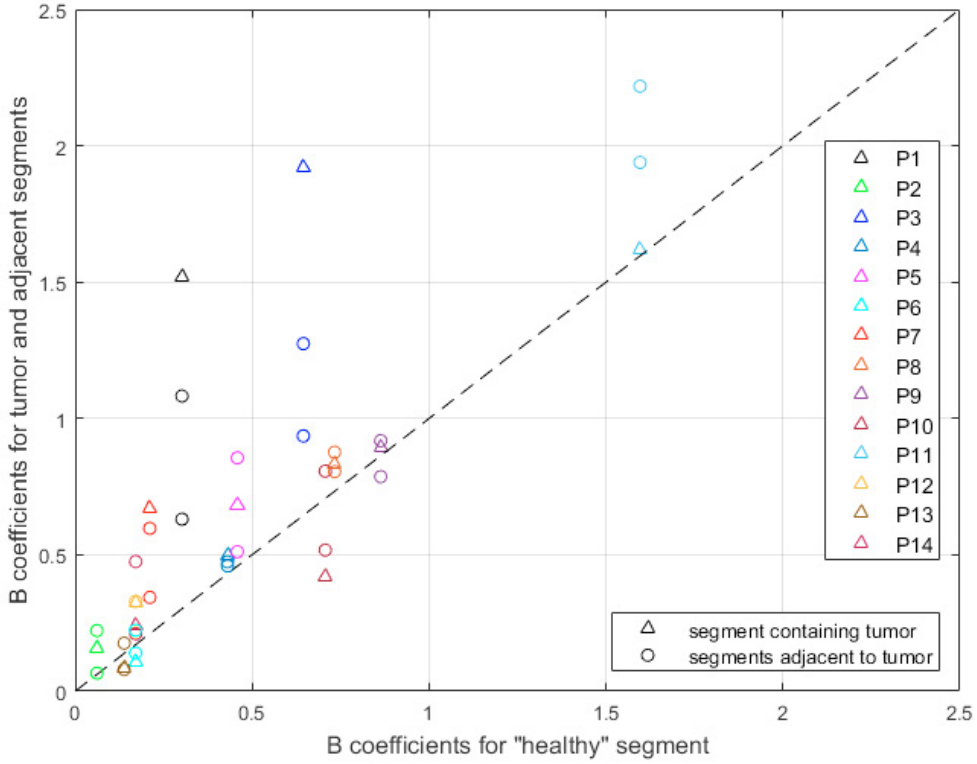

Fig. 6. Comparison of B coefficients in "healthy" and tumor segments for all subjects averaged across frequency, with points above the line indicating successful diagnostic of tumor presence

6. ACKNOWLEDGEMENTS

The authors acknowledge the support of Tiro Medical Ltd, Dr Richard Annand at Canterbury BreastCare and NZ National Science Challenge 7, Science for Technological Innovation (SfTI) as funded by the NZ Ministry for Business, Innovation and Enterprise.

REFERENCES

Abbas, S., Judit, Z., Donald, P., 2007. Elastic moduli of normal and pathological human breast tissues: an inversion-technique-based investigation of 169 samples. Physics in Medicine and Biology 52 (6), 1565.

Coughlin, S. S., Ekwueme, D. U., 2009. Breast cancer as a global health concern. Cancer epidemiology 33 (5), 315–318.

Elmore, J. G., Miglioretti, D. L., Reisch, L. M., Barton, M. B., Kreuter, W., Christiansen, C. L., Fletcher, S. W., 2002. Screening mammograms by community radiologists: variability in false-positive rates. Journal of the National Cancer Institute 94 (18), 1373–1380.

Heywang-Kbrunner, S. H., Hacker, A., Sedlacek, S., 2011. Advantages and Disadvantages of Mammography Screening. Breast Care 6 (3), 2–2.

Lotz, T., Muller, N., Hann, C. E., Chase, J. G., Feb. 2011. Minimal elastographic modeling of breast cancer for model based tumour detection in a Digital Image Elasto Tomography (DIET) System.

Peters, A., Chase, J. G., Van Houten, E. E., 2008. Digital image elasto-tomography: combinatorial and hybrid optimization algorithms for shape-based elastic property reconstruction. IEEE transactions on biomedical engineering 55 (11), 2575–2583.

Peters, A., Milsant, A., Rouz, J., Ray, L., Chase, J. G., Houten, E. E. W. V., 2004. Digital image-based elasto-tomography: Proof of concept studies for surface based mechanical property reconstruction. JSME International Journal Series C Mechanical Systems, Machine Elements and Manufacturing 47 (4), 1117–1123.

Peters, A., Wortmann, S., Elliot, R., Staiger, M., Chase, J., Van Houten, E. E., 2005. Digital Image-based Elasto-Tomography: First experiments in surface based mechancial property estimation of gelatine phantoms. JSME International Journal 48 (4), 562–569.

Petrov, A. Y., Docherty, P. D., Sellier, M., Chase, J. G., Jan. 2015. Multi-frequency Rayleigh damped elastography: in silico studies. Medical Engineering & Physics 37 (1), 55–67.

van den Ende, C., Oordt-Speets, A. M., Vroling, H., van Agt, H. M. E., Oct. 2017. Benefits and harms of breast cancer screening with mammography in women aged 40-49 years: A systematic review: Breast Cancer Screening in Women Aged 40-49 years. International Journal of Cancer 141 (7), 1295–1306.

Zhou, C., Chase, J. G., Ismail, H., Signal, M. K., Haggers, M., Rodgers, G. W., Pretty, C., 2018. Silicone phantom validation of breast cancer tumor detection using nominal stiffness identification in digital imaging elasto-tomography (DIET). Biomedical Signal Processing and Control 39, 435–447.